Available online at www.sciencedirect.com
SCIENCE DIRECT®
J. of Supercritical Fluids 35 (2005) 49–61
THE JOURNAL OF Supercritical Fluids
www.elsevier.com/locate/supflu

Citrus peel oil deterpenation with supercritical fluids Optimal process and solvent cycle design

S. Diaz[a], S. Espinosa[b], E.A. Brignole[a,*]

[a] *PLAPIQUI (Universidad Nacional del Sur-CONICET), Camino La Carrindanga Km 7, 8000 Bahia Blanca, Argentina*
[b] *Universidad Nacional del Comahue, Buenos Aires 1400, 8300 Neuquén, Argentina*

Received 20 July 2004; accepted 3 December 2004

Abstract

In this work supercritical deterpenation of orange peel oil with carbon dioxide is studied. Optimal schemes and operating conditions are determined through the formulation of a nonlinear programming model that includes reliable thermodynamic predictions with a group contribution equation of state and rigorous unit models. A detailed comparison of binary and ternary equilibrium predictions with available experimental data is reported. Simulation results are in agreement with previous laboratory-scale separation values. Different solvent cycle schemes have been included in the mathematical model. Net profit is maximized taking into account capital and operating costs associated to the complete deterpenation process. Numerical results show that a compression cycle is the optimal solvent recovery system in all cases. Furthermore, optimal operating conditions have been determined in main units (extractor and separator), for the production of both a five-fold concentrate and a high purity aroma, as raffinate, respectively.

Keywords: CO_2; Deterpenation; Optimization; Orange peel oil; Supercritical fluid processes

1. Introduction

Citrus essential oils are obtained from fruit peel by a "cold pressed" process and they are widely used in cosmetics, pharmaceuticals and food products. They are complex mixtures of more than 200 components, mainly hydrocarbon terpenes and oxygenated compounds, pigments, waxes, resins and flavonoids. Terpenes are unsaturated compounds that are readily decomposed by heat, light and oxygen and must be partially removed to avoid unpleasant flavors; they make up about 80–98 wt.% in most citrus peel oils. Oxygenated compounds constitute the flavor fraction that gives the characteristic citrus flavor. In orange peel oil, the main oxygenated compounds are linalool and decanal and the main terpenes are limonene and α-pinene. Lemon peel oil is mainly composed of citral, limonene and γ-terpinene.

Traditional processes for the deterpenation of citrus peel oils include steam distillation, vacuum distillation, extraction with liquid solvents and adsorption. Steam distillation leads to product degradation due to high temperatures. Vacuum distillation is preferable due to lower operating temperatures; however, an important fraction of aldehydes is lost with the consequent change in product quality. Extraction with organic solvents requires distillation to remove solvent residue with the risk of product thermal degradation. Chouchi et al. [1,2] have proposed a chromatographic adsorption/desorption process, using silica gel as adsorbent. Although this process renders high yields, it involves high-energy consumption at the desorption step and it is a semi-batch operation, not adequate for large scale processing.

Supercritical fluid fractionation by extraction (SFE) is an attractive alternative; it combines low operating temperatures, which prevents products from thermal degradation, and a benign solvent. In citrus oil deterpenation, the main issue

* Corresponding author. Tel.: +54 291 4861700x231; fax: +54 291 883 764.
E-mail addresses: sdiaz@plapiqui.edu.ar (S. Diaz), sespinos@uncoma.edu.ar (S. Espinosa), ebrignole@plapiqui.edu.ar (E.A. Brignole).

0896-8446/$ – see front matter © 2004 Elsevier B.V. All rights reserved.
doi:10.1016/j.supflu.2004.12.002

is to maintain desirable flavors and to minimize degradation that results in undesirable attributes such as bitterness [3]. A few authors have reported experimental data on pilot plant SFE deterpenation of citrus peel oils. These processes range from semibatch to simple countercurrent extraction with or without external reflux. Gerard [4] experimentally studied a countercurrent extraction column with external reflux and he proposed 80 bar and 333/343 K as operating pressure and temperature. Stahl and Gerard [5] concluded that deterpenation can be carried out at about 313 K, within a 70–80 bar pressure range, based on the solubility behavior of terpenes and sesquiterpenes. Sato et al. [6] reported the semibatch deterpenation of orange peel oil with supercritical carbon dioxide; they studied the effect of internal reflux induced by a temperature gradient in the column, on process selectivity and product recovery. Sato et al. [7] also reported laboratory-scale data for the continuous countercurrent extraction of terpenes from orange peel oil. Supercritical fluid fractionation of citrus peel oils with carbon dioxide was also experimentally studied by Reverchon et al. [8]. They analyzed countercurrent extraction with and without external reflux for different operating conditions (pressure, temperature and solvent-to-feed ratio) and extraction column packing, using a model mixture made up of two terpene hydrocarbons (limonene and γ-terpinene) and two oxygenated compounds (linalool and linalyl acetate).

More recently, Budich et al. [9] and Budich and Brunner [10] carried out a thorough study on the deterpenation of orange peel oil with supercritical carbon dioxide (SC-CO_2), reporting phase equilibrium data, countercurrent column experiments and flooding point measurements. They also formulated a simplified model, based on vapor–liquid equilibrium data, to perform stage calculations and a preliminary scale-up of the deterpenation process. The authors pointed out that further research is required in simulation and optimization to confirm scale-up calculations and to improve process efficiency.

In the design of chemical processes, the experimental task can be considerably reduced through the application of modeling, simulation and optimization techniques. Vapor–liquid equilibrium data for citrus peel oils with carbon dioxide has been correlated using cubic equations of state [7,11,12] and group contribution methods [13–15]. The modeling and optimization of the extraction and purification of natural products has been the subject of several studies in our group [16–19]. Recent work includes fractionation of fish oil fatty acid ethyl esters with SC-CO_2 [20,21] and citrus peel oil extraction optimization using different fractionation schemes and alternative supercritical fluids [15,22–24]. Most recently, Diaz et al. [25] have performed optimal solvent cycle and process design for lemon peel oil deterpenation, through the application of mixed integer nonlinear programming techniques.

In the present work, a nonlinear programming model is formulated for the simultaneous determination of operating conditions and process and solvent cycle scheme, including investment and operating costs for the entire process. The objective is the maximization of net profit, while fulfilling product recovery and purity specifications. Rigorous simulation models are included for process units. Phase equilibrium and heating, cooling and compression loads are provided by a group contribution equation of state (GC-EOS). Both binary and ternary vapor–liquid equilibrium predictions are compared to experimental data. Simulation results are also checked against pilot plant data [8–10].

2. Phase equilibrium and solubility predictions

Orange peel oil is a complex mixture of terpenes ($C_{10}H_{16}$) and sesquiterpenes ($C_{15}H_{24}$), oxygenated compounds and nonvolatile residues. However, it can be modeled as a binary mixture composed of limonene, as the main terpene compound, and linalool, representative of the oxygenated flavor fraction. Decanal is also present, almost in the same percentage as linalool, but linalool is selected due to the higher difficulty of its separation from limonene. Equilibrium predictions have been performed with the group contribution equation of state (GC-EOS) [29]. Pure group and interaction parameters for olefin groups [30]; revised carbon dioxide and aromatics binary interaction parameters [31] and carbon dioxide and paraffins binary interaction parameters [32] have been added to the original GC-EOS parameters. Moreover, an improved binary interaction parameter for carbon dioxide and the alcohol group has been determined to account for proximity effects between the ternary alcohol group and the olefinic group of linalool. This parameter has been estimated using vapor–liquid experimental data for the binary linalool–carbon dioxide [33]. With the new parameter, improved predictions of separation factors for orange oil components in CO_2 compared to reported experimental ones [7,10,34] have been obtained. The parameters used to model the system orange peel oil + carbon dioxide are presented in Appendix A.

As a first step, vapor pressure curves for limonene and linalool are compared to experimental data from Daubert and Danner [35] and Stull [36], in Fig. 1. Binary vapor–liquid equilibrium (VLE) calculations are plotted together with experimental data in Fig. 2 for the systems linalool + carbon dioxide and limonene + carbon dioxide. A good agreement has been found with experimental data; it should be noted that VLE results for limonene + carbon dioxide are completely predictive, while for linalool + carbon dioxide system, only one group interaction parameter has been adjusted.

Accurate terpene solubility estimations are necessary in order to obtain realistic modeling results. As shown in Fig. 3, the model provides a good prediction for the effect of pressure and temperature on limonene and linalool solubility in carbon dioxide. This is important because the low solubility below 8 MPa is used to separate the extracted components (mainly limonene) extracted at a pressure above 8 MPa by reducing pressure and temperature in the separator tank.

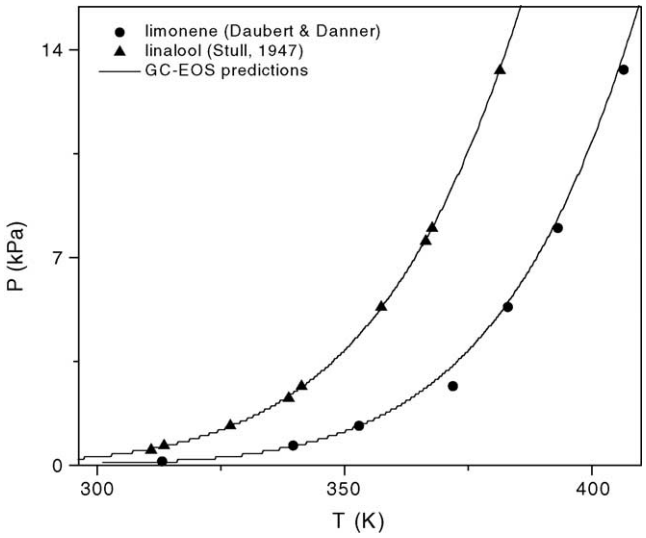

Fig. 1. Vapor-pressure of orange peel oil key components.

The quality of ternary predictions has also been verified. Figs. 4 and 5 compare GC-EOS predictions for the limonene + linalool + CO_2 mixture against experimental data [34] at 333 K and two different pressures (6.9 and 10 MPa). Additionally, Fig. 5 shows the quality of predictions for the component distribution ratio. Based on these results, calculated separation selectivity is in accordance with experimental results [7,34,37–39]. Predicted selectivity with GC-EOS, Peng–Robinson equation of state (PR-EOS) [40] and experimental data [7] at different temperatures and pressures are compared in Table 1. GC-EOS predictions are closer to experimental data and it is shown that selectivity decreases as the terpene/aroma ratio increases, making separation more difficult. It can be noted that a 0.1 change in selectivities is significant for selectivities lower than 2 in a 25-stage separation. GC-EOS ternary predictions, in good agreement with experimental data, indicate that the model is able to predict limonene–linalool interaction non-idealities. As it has been pointed out in previous work [11,12,39], significant errors can be made when binary, rather than ternary data, are used to obtain selectivities.

Fig. 6 shows a pressure-composition diagram for orange peel oil with CO_2. A few authors have reported experimental data on this system [10,41]. Continuous lines show our predictions with GC-EOS for a ternary mixture composed of carbon dioxide and orange oil, which has been modeled as

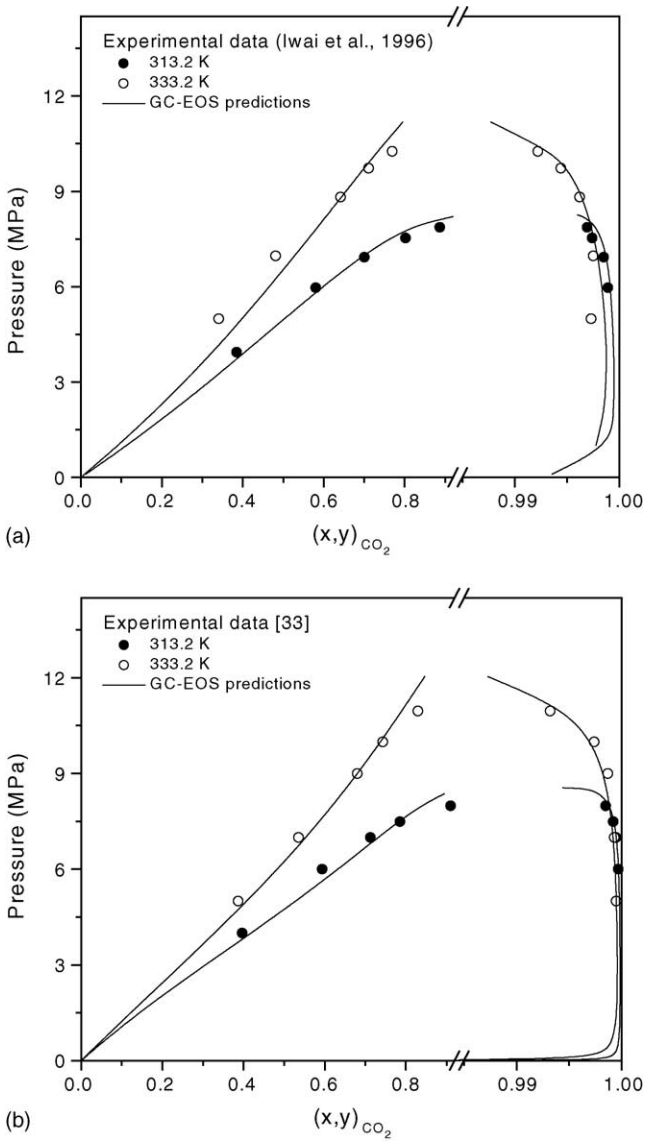

Fig. 2. Vapor–liquid equilibria for CO_2 + orange oil components binary mixtures.

98 wt.% limonene and 2 wt.% linalool. Fig. 6 supports the argument that orange peel oil can be properly modeled as a pseudo-binary mixture composed of limonene + linalool. Also, the estimated separation factors for limonene/linalool in the model mixture are in accordance with those of terpenes/aroma from orange oil experimental data [42].

Table 1
Limonene–linalool selectivity

T (K)	P (MPa)	Experimental data [7]	PR-EOS [7]	GC-EOS (this work 80/20 wt.%)	GC-EOS (this work 98/2 wt.%)
323	8.8	2.26	3.47	1.96	1.97
333	8.8	2.05	3.44	1.96	1.95
343	8.8	2.30	3.22	1.92	1.85
353	8.8	1.98	2.96	1.85	1.75
333	9.8	1.88	2.97	1.79	1.77

Comparison between experimental data and PR-EOS and GC-EOS thermodynamic models.

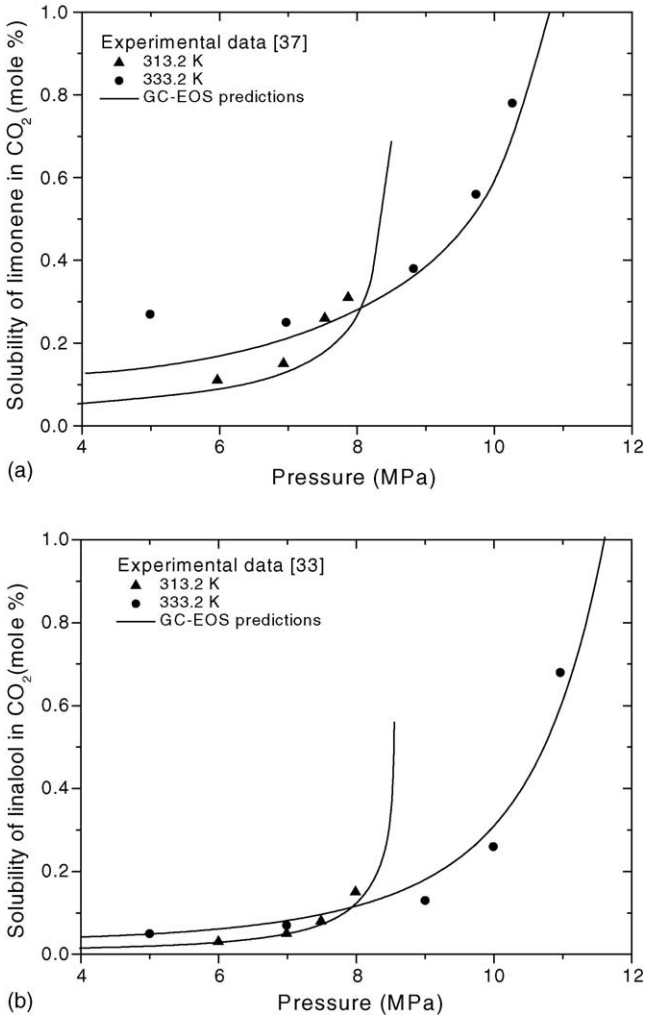

Fig. 3. Predictions and experimental data for limonene and linalool solubility in CO_2.

3. Process modeling and optimization

The selection of process schemes and operating conditions for supercritical fractionation closely follows the guidelines for design of conventional solvent extraction processes. One of the main differences is that the flow rate of the heavy phase is much larger than that of the feed because the near critical gas has a significant solubility in the liquid phase. In addition, in supercritical fluid fractionation, a large flow rate of solvent is required and the total flow rate of the extract phase is almost constant due to the relatively low solubility of the heavy components in the extract phase. The same can be applied to the raffinate phase. In a simplified analysis of deterpenation of essential oil, a simplified three component system can be considered as, for example: limonene (1), linalool (2) and CO_2 (3). Taking into account the constant flow rates of both phases, the process can be described as a linear cascade of stages. In this case, for a simple countercurrent operation scheme, the limiting recoveries of limonene and linalool (ϕ_1, ϕ_2) in the extract and raffinate, respectively, are determined by the relative volatility (α_{12}) between both components under the process conditions:

$$\alpha_{12} = \frac{\phi_1}{(1-\phi_2)}.$$

In the case of separation of limonene and linalool, this constraint limits the recovery and purity of the products obtained from the extraction column unless very inefficient operating conditions are chosen. For instance, if 80% recovery of component (1) in the extract and 80% recovery of component (2) in the raffinate are specified, the minimum required α_{12} value is 4. This relative volatility is obtained by operating at 5 MPa and 300 K. These conditions are close to the minimum solubility of terpenes in vapor phase, as it is shown in Fig. 3a and b, demanding larger flowrates for the separation. Similarly, if one operates at 333 K and 9 MPa α_{12} is 1.92 and if terpenes recovery in the extract is fixed at 80%, linalool recovery will be less than 60% in the raffinate. When the relative volatility between the components is low and the recoveries are high, the simple countercurrent extraction process is not feasible. This is even worse for systems such as orange oil in which the oxygenated fraction is dilute, because single-phase conditions are easily obtained. The use of reflux not only increases the purity and recoveries in the process, but introduces an additional design variable to keep the process within the two-phase region. From the point of view of phase equilibrium engineering, the first criteria for the initial specifications of the column is to compute the phase envelope for the average composition, determined by all feed streams to the extractor (essential oil, solvent and recycle), and check if the chosen operating conditions (pressure and temperature) are in the heterogeneous region. For example, the phase envelopes for two different feeds, with and without reflux, are shown in Fig. 7, where also the optimum conditions for the design of this extraction column are indicated. It can be seen that using the simple countercurrent case the optimum lies outside the heterogeneous region. Fig. 7 results correspond to an optimum design, for conditions that are presented in Table 4 in the next section.

3.1. Process description and simulation model

In a typical fractionation scheme, orange peel oil (modeled as a 98 wt.% limonene–2 wt.% linalool mixture) is fed to an extraction column in countercurrent with SC-CO_2. The aroma (linalool concentrate), saturated with CO_2, constitutes the raffinate. Limonene and carbon dioxide constitute the extract, which is expanded and sent to a separator tank. The recovered solvent is recycled to the extraction unit after compression or pumping.

The process mathematical model is solved within a sequential process simulator that includes rigorous models for a high-pressure multistage extractor [43] and a multiphase flash [44]. In these models, thermodynamic predictions

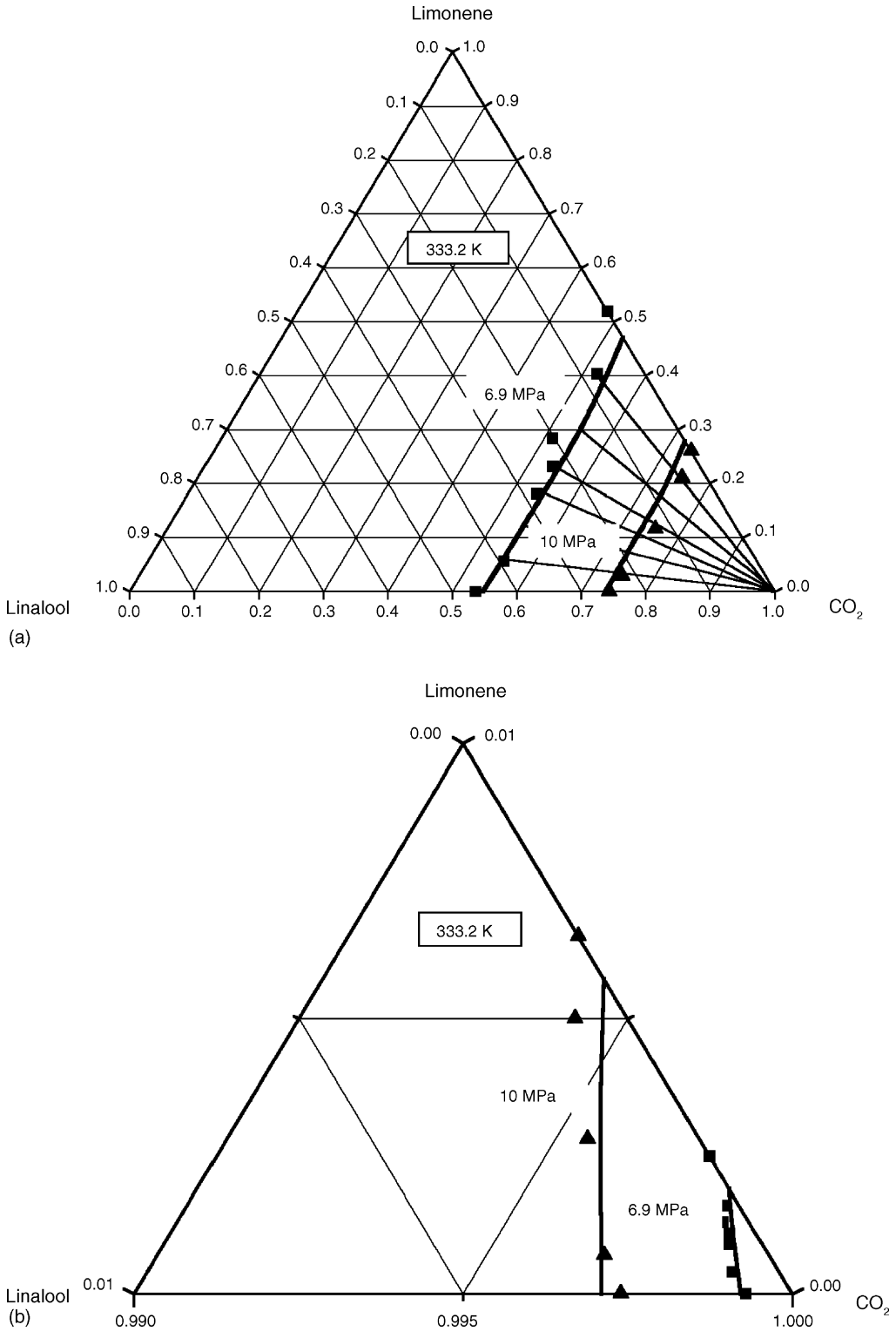

Fig. 4. Ternary plots for CO_2–limonene–linalool at 333 K: (a) heavy phase; (b) light phase. Symbols represent experimental data [34] and lines represents GC-EOS predictions.

are performed with the group contribution equation of state (GC-EOS). Compressor, pump, valve and heat exchanger models have been included to represent the solvent cycle.

3.1.1. Separation model

The extraction column is characterized by its diameter, number of stages and feed stage. The number of stages and size of the stripping section are strongly dependent on product

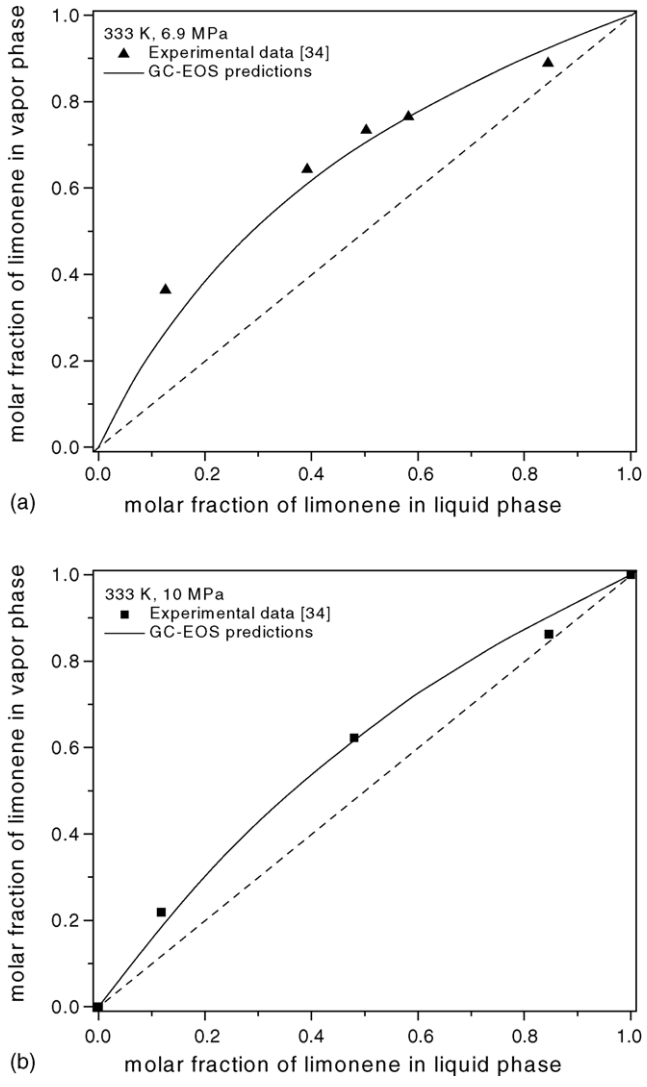

Fig. 5. Limonene distribution curve for the ternary system CO_2 + limonene + linalool at 333 K and two different pressures.

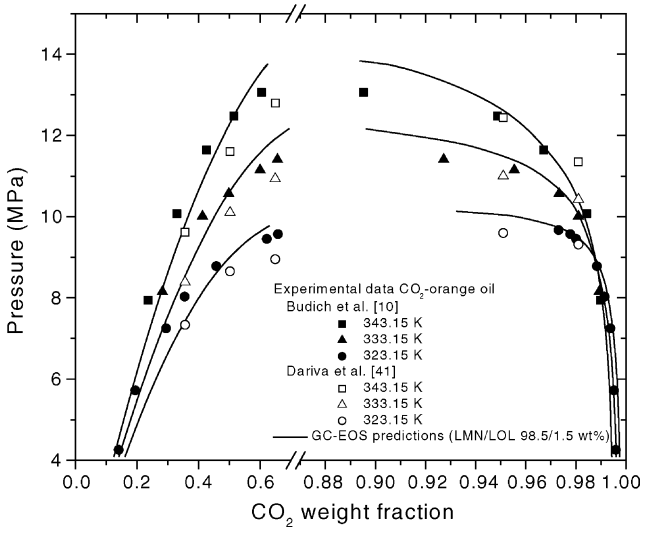

Fig. 6. GC-EOS predictions and experimental data for CO_2-orange peel oil.

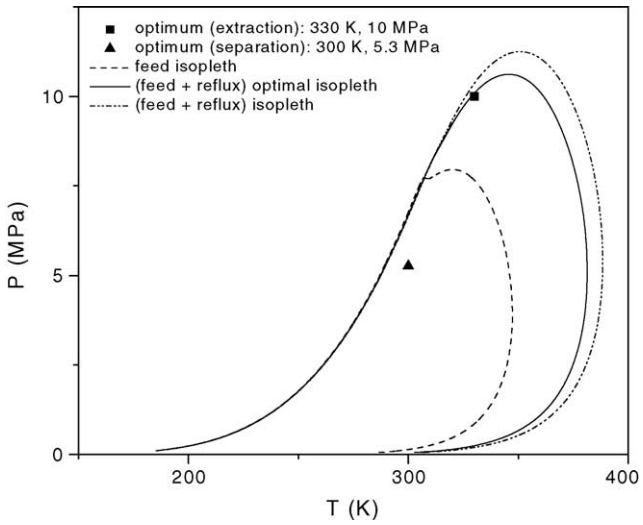

Fig. 7. Optimal solution on PT diagram. The optimal operating conditions belong to the heterogeneous region limited by isopleths with and without reflux.

purity specifications. Simulations have been carried out to obtain the minimum number of stages and optimum feed stage to achieve the purity specifications of the output streams. Therefore, these variables have been fixed in the process optimization model. This iterative technique allows reduction in the number of integer optimization variables and the corresponding problem complexity, without considerable loss of accuracy.

3.1.2. Hydraulic model

Column diameter of a packed column depends on the column flooding value under the process conditions. The use of correlations reported in the literature are not suitable for columns operating at near critical conditions and experimental data on pilot plant scale becomes necessary. Budich and Brunner [10] reported an extensive list of experimental flooding results for the extraction of orange peel oil with carbon dioxide at 323, 333 and 343 K and pressures ranging from 8 to 13 MPa. Based on these measurements, the authors [10] have given several correlations to estimate the minimum inner diameter of the column for a given packing factor. In the present work, both vapor and liquid phase densities have been calculated as a function of carbon dioxide density at column temperature and pressure through correlations reported by Budich and Brunner [10]. The experimental column capacity factor for the mixture CO_2 + orange oil correlation has also been calculated by a correlation developed by these authors [10]. A detailed description of flooding value calculation is given in Appendix B. The extractor diameter is calculated at 80% of flooding velocity.

3.1.3. Economic model

The economic model includes product sales and raw material, operating and investment costs. Net profit has been

Table 2
Utility costs

Natural gas	US$ 120.4/t
Cooling water	US$ 0.017/t
Low pressure steam	US$ 4/t
Electricity cost	US$ 0.068/kWh

calculated as:

$$\text{net profit} = \text{sales} - \text{raw material cost} - (\text{operating} + \text{investment})\,\text{costs},$$

where operating costs include electrical motor consumption, either as pump or compressor driver, cooling water and steam consumption. Utility costs are given in Table 2.

Process units are made of stainless steel due to the corrosive nature of citrus peel oil and carbon dioxide. Shell and tube heat exchangers and reciprocating pump capital costs curves have been obtained from Ulrich [26]. When current compressor capital costs are compared with those obtained from Ulrich [26], an over-estimation is observed, especially if a stainless steel unit is chosen. Consequently, the equations for the compressor cost have been correlated with the more realistic graphical data in Peters and Timmerhaus [27]. Capital cost curves for the extractor have been obtained from Institut Français du Pétrole [28]. Investment cost has been annualized considering a project life of 3 years. Orange peel oil cost is US$ 2/kg, high purity limonene, US$ 2.6/kg (Chemical Market Reporter, June 2003), and five-fold orange oil, US$ 33/kg (www.bestdeal.org, September 2003). Fold concentrate is defined as the mass ratio between feed and raffinate streams. Cost models for each unit are given in Appendix B.

3.2. Optimization model

The determination of an optimal solvent cycle scheme and operating conditions for the supercritical deterpenation of orange oil constitute a mixed integer nonlinear programming problem. Solvent cycle schemes have been embedded within a superstructure with binary variables associated to each potential unit. However, in order to explicitly compare the two alternative designs considered for the solvent recovery cycle (pumping or compressor mode), nonlinear programming (NLP) problems for fixed binary variables values have been solved.

Once again, the objective is to maximize net profit. Continuous optimization variables are: extraction pressure and temperature, pressure of the solvent recovery tank, solvent flow rate and reflux ratio. Most of the equality constraints that represent the process mathematical model, are solved within the sequential process simulator described in the previous section. Additional equality constraints have been added to the optimization problem to account for reflux convergence and the specification for 5- or 10-fold concentrate as raffinate. Inequality constraints include terpene purity specifications, solvent purity and operating bounds.

The deterpenation process and the solvent recovery system superstructure are shown in Fig. 8. The extract, mainly limonene and carbon dioxide, is heated before expanding through a Joule–Thomson valve to reduce solute solubility in SC-CO_2. The limonene + CO_2 stream is heated not further

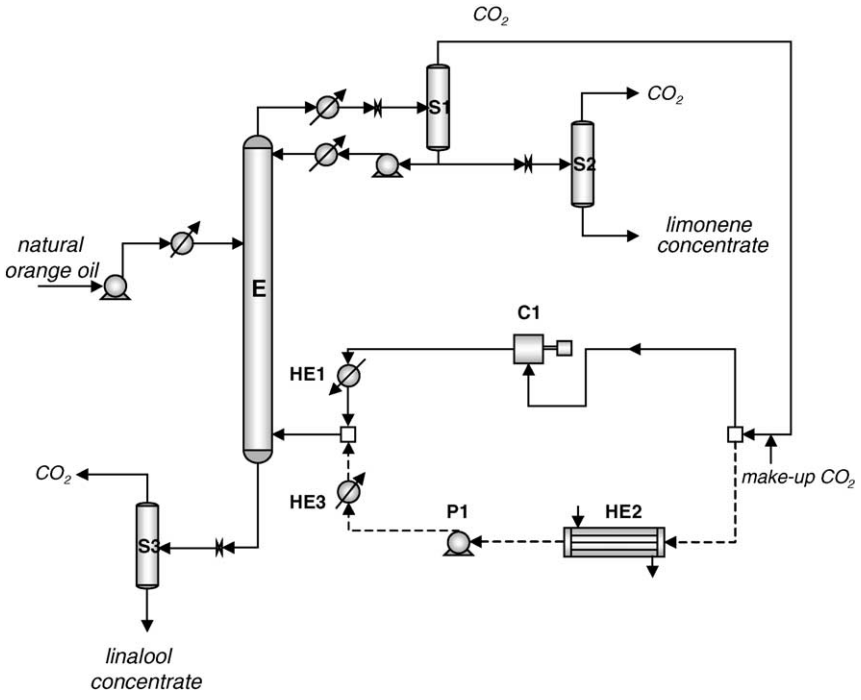

Fig. 8. Superstructure for supercritical deterpenation process and solvent recovery cycle.

than 10 °C to obtain conditions within the two-phase region, required by the optimization algorithm in the solvent recovery unit (S1). The vapor from this tank is the recovered solvent and the liquid is partly returned to the extractor as reflux and partly recovered as limonene product after a further expansion to ambient pressure. In compression mode, the recovered carbon dioxide is compressed (C1) to extraction pressure and then it is cooled to extraction temperature (HE1) with cooling water. In pump mode, the recovered solvent is condensed (HE2), pumped (P1) and heated (HE3) to extraction pressure and temperature, respectively. In this mode, a propane refrigeration cycle has been considered in order to condense carbon dioxide, and related capital costs curves have been implemented from Institut Français du Pétrole [28]; the solvent is heated in HE3 with low-pressure steam to extractor temperature. Nonlinear programming problems have been solved with a successive quadratic programming algorithm [45].

4. Discussion of results

4.1. Comparison of simulation results with laboratory-scale process data

The program can be alternatively used for process simulation or optimization. As a first step, our simulation results have been compared to laboratory-scale process data reported by Budich et al. [9]. A 25-stage countercurrent extraction column (P = 10 MPa, T = 333 K) with reflux has been simulated. The high-pressure separator is simulated at 5 MPa and 303 K. The entire set of conditions reported by Budich et al. [9] has been explored. Conditions required for the production of a five-fold concentrate are reported in Table 3, for an experimental solvent-to-feed ratio of 100.

As it is shown in Table 3, simulation results are in close agreement with laboratory plant data. Experimental data correspond to a solvent recovery cycle in pump mode, so simulation results for capital and operating costs are also reported for liquid carbon dioxide recycling. The proposed optimization model is able to determine new process operating conditions that maximize profit as a function of the fold value concentrate.

Table 3
Comparison between simulation results (this work) and pilot plant data [9]

Variable	Experimental data [9]	Simulation (this work)
Terpene purity (wt.%)	99.64	99.64
Terpene recovery (%)	81.13[a]	81.27
Aroma recovery (%)	83.54[a]	84.92
Aroma purity (wt.%)	7.31[a]	8.11
Solvent to feed ratio (mass)	100	107.85
Reflux ratio	–	1.24
Pumps consumption (kW)		5.35
Condenser area (m^2)		2.50
Heat exchanger area (m^2)		7.28
Capital cost (US$/kg product)		9.06
Operating cost (US$/kg product)		3.36
Profit (US$/kg product)		19.05[b]

Extraction: 10 MPa, T = 333 K; separation: 5 MPa, 303 K; 25 stage; feed stage: 11, 5-fold concentrate.
[a] Calculated from experimental data through mass balance.
[b] Limonene price (99.65 wt.% of purity) = US$ 2.12/kg.

4.2. Process and solvent cycle optimization for a five-fold raffinate

Thermodynamic predictions and process simulations have been favorably compared to experimental reported data. In this section, solvent cycle optimal design and process optimization have been performed. A 25 kg/h feed of the same 98 wt.% limonene and 2 wt.% linalool mixture is processed to obtain a five-fold orange peel oil concentrate. This specification has been included as an additional nonlinear equality constraint in the optimization problem. Inequality constraints impose a lower bound on linalool recovery (>90%), limonene purity in top product (>99.9 wt.%), and recycled solvent purity (>99.9 wt.%).

Optimization variables (extraction pressure and temperature, solvent recovery unit pressure and temperature, solvent flow rate and reflux ratio) and main process and economic variables are shown in Table 4, for both compression and pumping cycles. As compared to experimental data [9], the NLP optimum in pumping mode renders lower extractor temperature and pressure and lower temperature in the separation tank, together with a considerable decrease in solvent to feed ratio. These conditions lead to a significant increase in profit per product mass. Table 4 also shows that the optimal solvent cycle design corresponds to a solvent recovery system

Table 4
Continuous optimization variables and main costs for extraction at NLP optimum (25 kg/h feed, 25 theoretical stages, feed stage: 11, 5-fold concentrate)

Variable	NLP optimum	
	Compressor cycle	Pump cycle
Extractor pressure (MPa)	10	10
Extractor temperature (K)	330	330
Separator pressure (MPa)	5.25	5.44
Separator temperature (K)	300	301
Reflux ratio	2.47	2.45
Solvent-to feed ratio (mass)	149.95	153.48
Linalool in raffinate, CO_2 free (wt.%)	9.59	9.57
Linalool recovery (%)	95.94	95.87
Limonene in top product (wt.%)	99.90	99.90
Limonene recovery (%)	81.55	81.55
CO_2 in separator vapor (wt.%)	99.95	99.95
Extractor diameter (m)	0.26	0.26
Extractor height (m)	16.7	16.75
Flooding gas load (kg/(h m^2))	72437	72467
Compressor consumption (kW)	40.95	–
Pump consumption P1 (kW)	–	7.31
Condenser area HE2 (m^2)	–	2.87
Heat exchanger area (m^2)	9.92 (HE1)	9.35 (HE3)
Capital cost (US$/kg product)	5.92	10.29
Operating cost (US$/kg product)	0.57	4.03
Profit (US$/kg product)	27.06	19.24

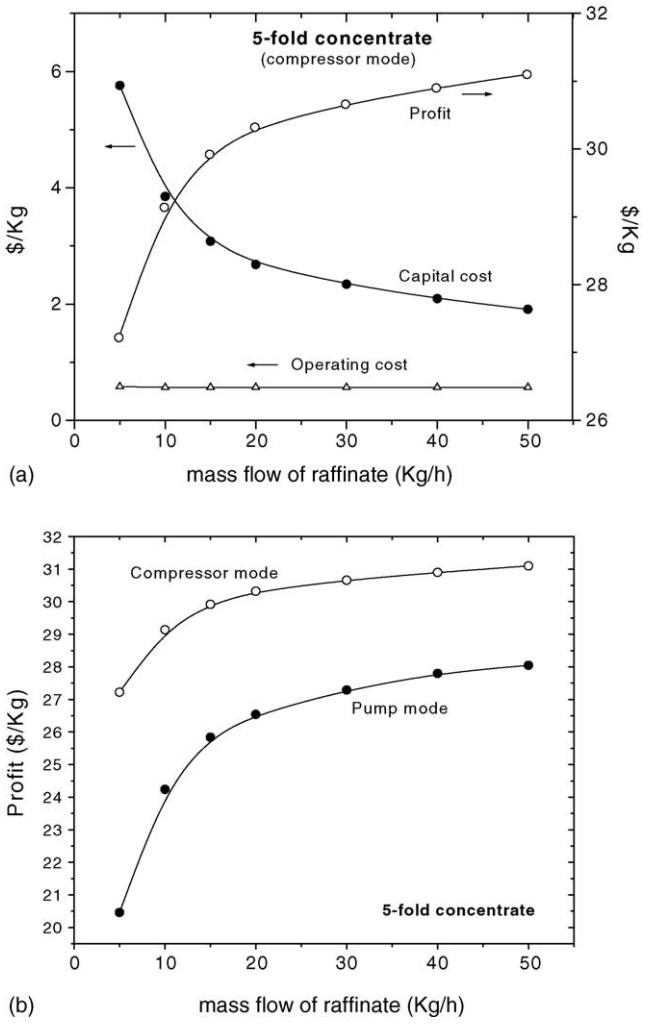

Fig. 9. Plant capacity optimization results to obtain 99.9 wt.% limonene purity in top product. (a) Compressor mode costs and profit for five-fold raffinate product; (b) comparison between compressor and pump mode profit for 5- and 10-fold raffinate product.

in compression mode. In this case, more than a 60% increase in profit has been obtained per unit of product mass. The convenience of using a compression cycle is in accordance with reported results based on an exergetic analysis that takes into account extractor and separator operating conditions [46].

Plant capacity has been analysed by comparing cost and maximum profit to obtain a 5- and 10-fold concentrate aroma and 99.9 wt.% limonene top product. Fig. 9a shows that operating costs are not affected by scale-up while capital costs decrease from US$ 5.92 to US$ 1.91/kg when plant capacity increases 10 times for a five-fold aroma concentrate (compressor mode for solvent recycle). Consequently, profit increases in the scale-up. Fig. 9b shows that the same trend is found in the production of a 10-fold concentrate. However, profit is more than 100% higher, mainly due to 10-fold product price. In this case, operating costs for compressor mode are around US$ 1.25/kg and capital costs are less than 50% higher than the required for a five-fold concentrate. Fig. 9b also reinforces the fact that maximum profit is obtained for a compression solvent cycle over a pump cycle.

Table 5
Nonlinear constraints for high purity orange oil recovery

Nonlinear constraint	Lower bound
Linalool purity (CO_2 free) (mol%)	99.00
Linalool recovery (%)	90.00
Limonene purity (CO_2 free) (mol%)	99.00
Carbon dioxide in vapor (mol%)	99.97

4.3. Process and solvent cycle optimization for high-purity orange oil recovery

The determination of optimal operating conditions for a 99 wt.% linalool purity product has been performed with the current optimization model. Due to uncertainties in high-purity product market price, the objective function has been total cost minimization. Bounds for nonlinear constraints are shown in Table 5. A larger number of stages are necessary to achieve the required separation. In previous work [15], optimal operating conditions for the aroma extraction were determined from a model mixture limonene/linalool 80/20 wt.%. Separation in this case was rather simple, requiring less rigorous extraction conditions.

Table 6 shows optimization results and cost values to process 25 kg/h of orange peel oil (98 wt.% limonene and 2 wt.% linalool). An important reduction in pressure is obtained in the separation tank, which is directly associated to an increase in compression cost. To reduce compression energy consumption (147.26 kW), a two-stage compression step with intermediate refrigeration has also been explored which renders a 20% decrease in compression work and 18% in cost.

Table 6
Continuous optimization variables and main costs for the countercurrent extraction with reflux at solvent cycle NLP optimum (25 kg/h feed, 28 theoretical stages, feed stage: 11, high-purity aroma)

Variable	NLP optimum (compressor cycle)
Feed (kg/h)	25
Extractor pressure (MPa)	10
Extractor temperature (K)	334.06
Separator pressure (MPa)	2.23
Separator temperature (K)	270.80
Reflux ratio	2.27
Solvent-to-feed ratio (mass)	183.73
Linalool in raffinate, CO_2 free (wt.%)	98.18
Linalool recovery (%)	94.89
Limonene in top product (wt.%)	99.90
Limonene recovery (%)	99.96
Extractor diameter (m)	0.28
Extractor height (m)	19.14
Compressor consumption (kW)	147.26
Heat exchanger area HE1 (m^2)	16.31
Capital cost (US$/kg product)	90.62
Operating cost (US$/kg product)	22.18
Profit (US$/kg product)	299.33

However the capital cost, for unit of concentrated linalool (98%), is still nine times higher than the capital cost value (Table 4) of a five-fold concentrate, this results justify the use of a concentrated linalool feed to obtain high purity linalool.

5. Conclusions

The integration of thermodynamic modeling with group contribution methods and nonlinear programming techniques provides an efficient tool for the optimal design and scale-up of supercritical extraction processes. The group contribution equation of state (GC-EOS) constitutes a robust support for simulation and optimization models. Comparison with pilot plant data has confirmed the potential of the simulation model. The integration of this rigorous model to a mathematical programming algorithm and the inclusion of an economic model have allowed optimization of process and solvent cycle operating conditions to achieve maximum net profit. High solvent flow rate and reflux-ratio together with a larger stripping section, have been necessary to obtain a five-fold product concentrate. The production of high purity aroma (98 wt.%) has required more theoretical stages and larger differences between extractor and separator operating conditions. Comparison of results with previous work on a model mixture limonene/linalool 80/20 wt.% shows that extraction is increasingly difficult as the ratio limonene/linalool increases, due to the mixture separation factor reduction.

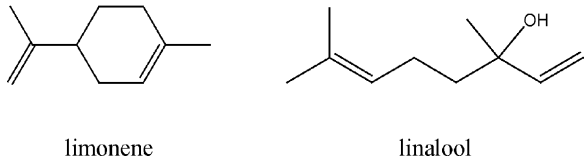

Fig. A.1. Chemical structures of orange oil key components.

Table A.1
Critical properties for components (D_c: critical diameter)

Component	T_c (K)	P_c (MPa)	T_b (K)	Molecular weight	D_c (cm/mol)
CO_2	304.2	7.280	–	44.00	3.1289
Limonene	660.0	2.750	449.65	136.2	5.6027
Linalool	630.5	2.388	471.15	154.4	6.1712

Finally, a comparison of optimization results between two different solvent cycle designs (pump and compressor) has determined that a compression cycle is the most cost-effective alternative for the required process operating conditions.

Appendix A. Component physical properties and GC-EOS interaction parameters

Chemical structures of orange oil key components are shown in Fig. A.1.

Critical properties and GC-EOS interaction parameters are listed in Tables A.1–A.4.

Table A.2
Pure group parameters

Group	T^* (K)	q	g^*	G'	g''	CO_2	Limonene	Linalool
CH_2	600	0.54	356080	−0.8755	0	0	0	2
C═CH	600	0.676	546780	−1.0966	0	0	0	1
CH═CH_2	600	1.176	337980	−0.6764	0	0	0	1
CH_3(B)/$WSCH_3$(B)	600	0.7891	316910	−0.9274	0	0	1	3
$CYCH_2$	600	0.54	466550	−0.6062	0	0	3	0
CYCH	600	0.228	466550	−0.6062	0	0	1	0
ACH	600	0.4	723210	−0.606	0	0	1	0
C═CH_2	600	0.988	323440	−0.6328	0	0	1	0
$ACCH_3$	600	0.968	506290	−0.8013	0	0	1	0
COH[a]	512.6	0.7138	1207500	−0.6441	0	0	0	1
CO_2	304.2	1.261	531890	−0.578	0	1	0	0

[a] Tertiary alcohol joined to an olefinic group.

Table A.3
Binary interaction parameters (above diagonal) and temperature dependence of binary interaction parameters (below diagonal)

Group	CH_2	C═CH	CH═CH_2	CH_3(B)	$CYCH_2$	CYCH	ACH	C═CH_2	$ACCH_3$	COH	CO_2
CH_2	1	0.977	0.977	1	1	1	1.041	1	0.975	0.682	0.874
C═CH	0	1	1.094	0.977	1	1	1	1.094	1.040	0.773	1
CH═CH_2	0	0	1	0.977	1	1	0.984	1.094	1.034	1.04	0.948
CH_3(B)	0	0	0	1	1	1	1.041	1	0.975	0.715	0.898
$CYCH_2$	0	0	0	0	1	1	0.98	1.040	0.994	0.719	0.928
CYCH	0	0	0	0	0	1	0.98	1.040	0.994	0.719	0.928
ACH	0.094	0	0	0.094	0	0	1	1.040	1.007	0.826	1.060
C═CH_2	0	0	0	0	0	0	0	1	1.040	0.769	1.057
$ACCH_3$	0	0	0	0	0	0	0	0	1	0.774	0.938
COH	0	0	0	0	0	0	0	0	0	1	0.785
CO_2	0	0	0	0	0.21	0.21	0	0	0	0	1

Table A.4
Binary nonrandomness parameters

Group	CH_2	C=CH	$CH{=}CH_2$	CH_3(B)	$CYCH_2$	CYCH	ACH	$C{=}CH_2$	$ACCH_3$	COH	CO_2
CH_2	0	0	0	0	0	0	0.392	0	0	1.471	4.683
C=CH	0	0	0	0	0	0	0	0	0	1.376	0
$CH{=}CH_2$	0	0	0	0	0	0	0	0	0	0	0
CH_3(B)	0	0	0	0	0	0	0.392	0	0	1.471	4.683
$CYCH_2$	0	0	0	0	0	0	0	0	0	1.471	0
CYCH	0	0	0	0	0	0	0	0	0	1.471	0
ACH	0.392	0	0	0.392	0	0	0	0	0	4.091	−6.888
$C{=}CH_2$	0	0	0	0	0	0	0	0	0	0.603	0
$ACCH_3$	0	0	0	0	0	0	0	0	0	0.784	−14.93
COH	10.22	1.376	0	10.22	10.22	10.22	20.74	0.603	20.74	0	0.22
CO_2	4.683	0	0	4.683	0	0	−3.329	0	−3.94	−1.18	0

Appendix B. Cost correlations and flooding point calculation

Investment cost correlations are in US$/h. Estimations are based on 8000 h/y (cost indexes: I_{CE}, for correlations from Ulrich [26], $I_{Marshall}$, for correlations from Peters and Timmerhaus [27]).

B.1. Compressor cost (from [27])

Installed cost of stainless-steel compressors

$$C_{compr} = \frac{I_{Marshall}}{256} \times (-0.11013 + 0.1661 \times {W_s}^{0.65655}),$$

where W_s (kW) stands for shaft work.

B.2. Pumps costs (from [26])

Installed cost for CO_2 pump:

$$C_{pump} = \frac{I_{CE}}{315} \times (0.9469 + 0.1324 \times W_s) \times (-1.8647 + 5.2197 \times p^{0.1512}),$$

where W_s is shaft work (kW) and p stands for pressure (atm).

For feed and reflux pumps:

$$C_{pump} = \frac{I_{CE}}{315} \times (0.1560 + 0.9033 \times {W_s}^{0.468}) \times (-1.8647 + 5.2197 \times p^{0.1512}),$$

where $0.01 < W_s < 20$ kW.

B.3. CO_2 heat exchangers (from [26])

$$C_{hex} = \frac{I_{CE}}{315} \times (0.1666 + 0.0506 \times A^{0.67613}) \times (5.2428 + 0.5931 \times p^{0.2935}),$$

where A is heat exchange area (m^2).

B.4. Extractor and separator (from [28]):

$$C_{extractor} = 1.15 \times \left(\frac{I_{CE}}{182.1} \times (C_{shell+heads} \times 2.9 \times f_e + C_{access}) + C_{packing} \right) f_p,$$

with $C_{shell+heads} = \text{weight} \times (2 - \log D)$,

where c_p is shell cost, f_m the correction factor for material (=2.9 for ss316), f_e the correction factor for thickness, f_p the pressure correction factor, C_{access} the accessories cost, D the column diameter (m), $C_{packing}$ the packing cost, 1.15 stands for installation costs. Packing cost has been calculated from design curves (Sulzer Chemtech USA Inc., April 2001).

Extractor diameter has been calculated from the continuity equation, at 80% of flooding.

$$D = \frac{4 \times V_{max} M_g}{\pi \times \rho_g \times 0.8 \times u_{s,g}},$$

where V_{max} is the maximum vapor flow and M_g the gas molecular weight.

Flooding velocity has been calculated through:

$$u_{s,g} = F_V \times \left(\frac{\rho_l - \rho_g}{\rho_g} \right)^{0.5},$$

where F_V is the column capacity factor, which has been calculated with an empirical correlation developed by Budich and Brunner [10] for the carbon dioxide and orange peel oil mixture:

$$F_V = \frac{1}{(8 + 60\psi^{0.5})},$$

vapor and liquid phase density, ρ_l and ρ_v, have been also calculated as function of carbon dioxide density at column temperature and pressure using the following correlations, also developed by Budich and Brunner [10]:

$$\rho_g = 1.122\rho_{CO_2} - 0.001606\rho_{CO_2}^2 + 5.317 \times 10^{-6}\rho_{CO_2}^3 \text{ (kg/m}^3\text{)},$$

$$\rho_l = \frac{(1859.45 - 3T) - (8.2176 - 0.01851T)\rho_{CO_2}}{1 - (0.00597 - 1.1 \times 10^{-5}T)\rho_{CO_2}} \; (T \text{ in K; kg/m}^3),$$

and the flow parameter, ψ has been calculated as:

$$\psi = \frac{L \times M_L}{V_{max} \times M_g} \sqrt{\frac{\rho_g}{\rho_l}}.$$

Column height has been estimated as:

$$H = \frac{N_t}{N_m},$$

where N_t is the number of theoretical stages per meter (based on design packing curves) and N_m the number of calculated theoretical stages.

A vertical vessel has been selected for the separation tank.

B.5. CO_2 condenser refrigeration cost

Refrigeration temperature = 250 K.

References

[1] D. Chouchi, D. Barth, R.M. Nicoud, Fractionation of citrus cold-pressed oils by supercritical CO_2 desorption, in: M. Perrut, G. Brunner (Eds.), Proceedings of the Third International Symposium on Supercritical Fluids, vol. 2, 1994, p. 183.

[2] D. Chouchi, D. Barth, E. Reverchon, G. Della Porta, Supercritical CO_2 desorption of bergamot peel oil, Ind. Eng. Chem. Res. 34 (1995) 4508.

[3] F. Temelli, C.S. Chen, R.J. Braddock, Supercritical fluid extraction in citrus oil processing, Food Technol. 6 (1988) 145.

[4] D. Gerard, Continuous removal of terpenes from essential oils by countercurrent extraction with compressed carbon dioxide, Chem. Ing. Technol. 56 (1984) 794.

[5] E. Stahl, D. Gerard, Solubility behavior and fractionation of essential oils in dense carbon dioxide, Perfumer Flavorist 10 (1985) 29.

[6] M. Sato, M. Goto, T. Hirose, Fractional extraction with supercritical carbon dioxide for the removal of terpenes from citrus oil, Ind. Eng. Chem. Res. 34 (1995) 3941.

[7] M. Sato, M. Goto, T. Hirose, Supercritical fluid extraction on semi-batch mode for the removal of terpene in citrus oil, Ind. Eng. Chem. Res. 35 (1996) 1906.

[8] E. Reverchon, A. Marciano, M. Poletto, Fractionation of peel oil key mixture by supercritical CO_2 in a continuous tower, Ind. Eng. Chem. Res. 36 (1997) 4940.

[9] M. Budich, S. Heilig, T. Wesse, V. Leibkuchler, G. Brunner, Countercurrent deterpenation of citrus oil with supercritical CO_2, J. Supercrit. Fluid 14 (1999) 105.

[10] M. Budich, G. Brunner, Vapor–liquid equilibrium data and flooding point measurements of the mixture carbon-dioxide + orange peel oil, Fluid Phase Equilibr. 158–160 (1999) 759.

[11] A. Bertucco, G.B. Guarise, A. Zandegiacomo Riziò, Binary and ternary vapor–liquid equilibrium data for the system CO_2–limonene–linalool, in: Proceedings of the Fourth Italian Conference on Supercritical Fluids and their Applications, 1997, p. 83.

[12] S.A.B. Vieira de Melo, G.M.N. Costa, A.M.C. Uller, F.L.P. Pessoa, Modeling high-pressure vapor–liquid equilibrium of limonene, linalool and carbon dioxide systems, J. Supercrit. Fluids 16 (1999) 107.

[13] F. Temelli, J. O'Connell, C. Chen, R. Braddock, Thermodynamic analysis of supercritical carbon dioxide extraction of terpenes from cold-pressed orange oil, Ind. Eng. Chem. Res. 29 (1990) 618.

[14] E. Hypek, L.H.M. Silva, E. Batista, D.S. Marques, M.A.A. Meireles, A.J.A. Meirelles, in: L.T. Pinto (Ed.), Proceedings of the Second Mercosur Congress on Process Systems Engineering (abstracts), 1999, p. 667.

[15] S. Espinosa, S. Diaz, E. Brignole, Optimal design of supercritical fluid processes, Comp. Chem. Eng. 24 (2000) 1301.

[16] S. Espinosa, S. Bottini, E. Brignole, Process analysis and phase equilibria for the removal of chemicals from fatty oils using near critical solvents, Ind. Eng. Chem. Res. 39 (2000) 3024.

[17] S. Espinosa, S. Diaz, E. Brignole, Biomolecules supercritical extraction: process simulation and optimization, in: Proceedings of the AIChE Annual Meeting, 2000 (CD).

[18] S. Diaz, H. Gros, E. Brignole, Thermodynamic modeling, synthesis and optimization of extraction-dehydration processes, Comp. Chem. Eng. 24 (2000) 2069.

[19] H. Gros, S. Diaz, E. Brignole, Process synthesis and optimization of near critical separations of aqueous azeotropic mixtures, J. Supercrit. Fluids 12 (1998) 69.

[20] S. Diaz, S. Espinosa, E. Brignole, Modeling and simulation tools for supercritical fluid processes, Comput. Aid. Process Eng. 8 (2000) 319.

[21] S. Espinosa, S. Diaz, E. Brignole, Thermodynamic modeling and process optimization of supercritical fluid fractionation of fish oil fatty acid ethyl esters, Ind. Eng. Chem. Res. 41 (2002) 1516.

[22] S. Espinosa, S. Diaz, E. Brignole, High pressure extraction with alternative supercritical fluids. Thermodynamic modeling and process optimization, Chem. Eng. Trans. 3 (2003) 419.

[23] S. Espinosa, S. Diaz, E. Brignole, Phase equilibria and process optimization for the deterpenation of citrus peel oil with near critical CO_2 and ethane, in: Proceedings of the AIChE Spring National Meeting, 2003 (CD).

[24] S. Espinosa, S. Diaz, E. Brignole, High pressure extraction with alternative supercritical fluids. Thermodynamic modeling and process optimization, Chem. Eng. Trans. 3 (2003) 419.

[25] S. Diaz, S. Espinosa, E. Brignole, Optimal solvent cycle design in supercritical fluid processes, Latin Am. Appl. Res. 33 (2003) 161.

[26] G.D. Ulrich, A Guide to Chemical Engineering Process Design and Economics, Wiley, NY, 1984.

[27] M.S. Peters, K.D. Timmerhaus, Plant Design and Economics for Chemical Engineers, McGraw-Hill, NY, 1991.

[28] Institut Français du Pétrole, Manual of Economic Analysis of Chemical Processes, McGraw-Hill, France, 1981.

[29] S. Skjold-Jorgensen, Group contribution equation of state (GC-EOS): a predictive method for phase equilibrium computations over wide ranges of temperatures and pressures up to 30 MPa, Ind. Eng. Chem. Res. 27 (1988) 110.

[30] J. Pusch, J. Schmelzer, Extension of the group-contribution equation of state parameter matrix for the prediction of phase equilibria containing argon, ammonia, propene and other alkenes, Ber. Bunsenges, Phys. Chem. 97 (1993) 597.

[31] A. Bamberger, J. Schmelzer, D. Walther, G. Maurer, High-pressure vapour–liquid equilibria in binary mixtures of carbon dioxide and benzene compounds and their correlation with the generalized Bender and Skjold-Jorgensen's group contribution equation of state, Fluid Phase Equilibr. 97 (1994) 167.

[32] S. Espinosa, G. Foco, A. Bermúdez, T. Fornari, Revision and extension of the group contribution equation of state to new solvent groups and higher molecular weight alkanes, Fluid Phase Equilibr. 172 (2000) 129.

[33] Y. Iwai, N. Hosotani, T. Morotomi, Y. Koga, Y. Arai, High pressure vapor–liquid equilibria for carbon dioxide + linalool, J. Chem. Eng. Data 39 (1994) 900.
[34] T. Morotomi, Y. Iwai, H. Yamaguchi, Y. Arai, High-pressure vapor–liquid equilibria for carbon dioxide + limonene + linalool, J. Chem. Eng. Data 44 (1999) 1370.
[35] T.E. Daubert, R.P. Danner, Physical and Thermodynamic Properties of Pure Chemicals: Data Compilation, Hemisphere Publishing Corporation, 1989.
[36] D.R. Stull, Vapor pressure for pure substances: organic compounds, Ind. Eng. Chem. 39 (1947) 517.
[37] Y. Iwai, T. Morotomi, Y. Koga, K. Sacamoto, Y. Arai, High pressure vapor–liquid equilibria for carbon dioxide + limonene, J. Chem. Eng. Data 41 (1996) 951.
[38] J. Fonseca, P.C. Simoes, M. Nunes da Ponte, An apparatus for high-pressure VLE measurements using a static mixer. Results for (CO_2 + limonene + citral) and (CO_2 + limonene + linalool), J. Supercrit. Fluids 25 (2003) 7.
[39] S.A.B. Vieira de Melo, P. Pallado, G.B. Guarise, A. Bertucco, High-pressure vapor–liquid equilibrium data for binary and ternary systems formed by supercritical CO_2, limonene and linalool, Braz. J. Chem. Eng. 16 (1999) 7.
[40] D.Y. Peng, D.B. Robinson, A new cubic equation of state, Ind. Eng. Chem. Fund. 15 (1976) 59.
[41] C. Dariva, G.R. Ribeiro, J.V. Oliveira, Equilibrio de Fases a Altas Pressões para o Sistema CO_2—Óleo de Naranja, in: Proceedings of the Fifth International Conference EQUIFASE99, vol. 1, Vigo-España, 1999, pp. 139–145.
[42] G. Brunner, Industrial process development. countercurrent multistage gas extraction (SFE) processes, J. Supercrit. Fluids 13 (1998) 283.
[43] E.A. Brignole, P.M. Andersen, Aa. Fredenslund, Supercritical fluid extraction of alcohols from water, Ind. Eng. Chem. Res. 26 (1987) 254.
[44] M.L. Michelsen, The isothermal flash problem. Part II. Phase-split calculation, Fluid Phase Equilibr. 9 (1982) 21–40.
[45] L. Biegler, J. Cuthrell, Improved infeasible path optimization for sequential modular simulators. II: the optimization algorithm, Comp. Chem. Eng. 9 (1985) 257.
[46] R.L. Smith, H. Inomata Jr., M. Kanno, K. Arai, Energy analysis of supercritical carbon dioxide extraction processes, J. Supercrit. Fluids 15 (1999) 145.